Three-Dimensional Structure of the FK506 Binding Protein/Ascomycin Complex in Solution by Heteronuclear Three- and Four-Dimensional NMR†

Robert P. Meadows, David G. Nettesheim, Robert X. Xu, Edward T. Olejniczak, Andrew M. Petros, Thomas F. Holzman, Jean Severin, Earl Gubbins, Harriet Smith, and Stephen W. Fesik*

Pharmaceutical Discovery Division, Abbott Laboratories, Abbott Park, Illinois 60064

Received September 11, 1992; Revised Manuscript Received October 28, 1992

ABSTRACT: A high-resolution three-dimensional solution structure of the FKBP/ascomycin complex has been determined using heteronuclear multidimensional nuclear magnetic resonance spectroscopy (NMR) and a distance geometry/simulated annealing protocol. A total of 43 structures of the complex, including 3 tightly bound water molecules, were obtained using 1958 experimental restraints consisting of 1724 nuclear Overhauser effect (NOE) derived distances, 66 χ^1 and 46 ϕ angular restraints, and 122 hydrogen bond restraints. The root mean square (rms) deviations between the 43 FKBP/ascomycin solution structures and the mean atomic coordinates were 0.43 ± 0.08 Å for the backbone heavy atoms and 0.80 ± 0.08 Å for all non-hydrogen atoms. Angular order parameters for the family of 43 conformations were calculated to determine dihedral convergence. Order parameters for ϕ, ψ, and χ^1 angles exhibited mean values of 0.98, 0.97, and 0.95, respectively, while the mean of the χ^2 order parameter was 0.63. Comparisons were made between the FKBP/ascomycin complex and two NMR-derived solution structures of unbound FKBP and the X-ray crystal structure of an FKBP/FK506 complex. Differences were observed between the FKBP/ascomycin complex and uncomplexed FKBP for residues 33–45 and 78–92. In contrast, the NMR-derived solution structure of the FKBP/ascomycin complex and the X-ray crystal structure of the FKBP/FK506 complex were very similar. Differences between the two complexes were mainly observed in the conformations of some highly solvent exposed side chains.

FK506 (Figure 1) is a potent immunosuppressant that acts by binding to a 107 amino acid protein, FK-binding protein (FKBP).[1] Although FKBP is a peptidylprolyl *cis–trans*-isomerase (PPIase) that is inhibited by FK506 (Siekierka et al., 1989; Harding et al., 1989), PPIase inhibition does not appear to be the cause of immunosuppression (Bierer et al., 1990; Schreiber, 1991). Rather, recent evidence suggests that the immunosuppressive activities displayed by FK506 are due to the binding and inhibition of the calcium- and calmodulin-dependent phosphatase, calcineurin, by the FKBP/FK506 complex (Liu et al., 1991). Despite the 10–100-fold increase in potency observed for FK506 compared to the clinically well-established immunosuppressant cyclosporin A (CsA) (Yoshimura et al., 1989), the toxic side effects observed for FK506 (Fung et al., 1991) may limit its clinical utility.

Structural information on FKBP/immunosuppressant complexes and their interaction with calcineurin could aid in the discovery of more potent and potentially less toxic immunosuppressants. Three-dimensional structures of FKBP/FK506 (Van Duyne et al., 1991a) and FKBP complexed to the immunosuppressant rapamycin (Figure 1) (Van Duyne et al., 1991b) have been obtained by X-ray crystallography. The structures of the two complexes were found to be very similar, except for regions involved in either a large number of crystal contacts or a very different number of contacts

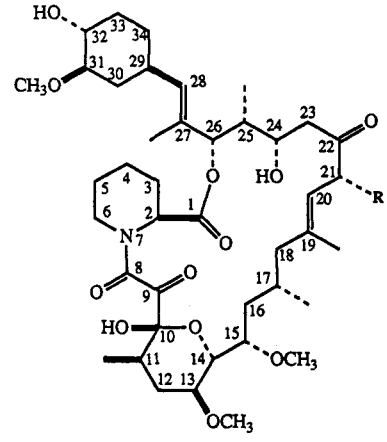

FK506 R= $CH_2CH{=}CH_2$
Ascomycin R= CH_2CH_3
35 36

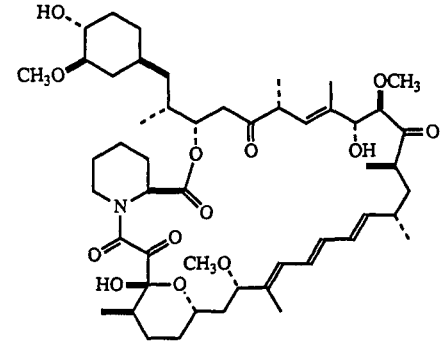

Rapamycin

FIGURE 1: Primary structure of FK506, ascomycin, and rapamycin.

(Van Duyne et al., 1993). In addition, the X-ray structures of FKBP with bound immunosuppressants were similar to

† This research was funded in part by the National Institute of General Medical Sciences (GM45351, awarded to S.W.F.).

* To whom correspondence should be addressed.

[1] Abbreviations: FKBP, FK506 binding protein; PPIase, peptidylprolyl *cis–trans*-isomerase; CsA, cyclosporin A; NMR, nuclear magnetic resonance; NOE, nuclear Overhauser effect; NOESY, nuclear Overhauser effect spectroscopy; HMQC, heteronuclear multiple-quantum coherence; HSQC, heteronuclear single-quantum coherence; DG, distance geometry; SA, simulated annealing; 2D, two dimensional; 3D, three dimensional; 4D, four dimensional; ppm, parts per million; rmsd, root mean square deviations.

0006-2960/93/0432-754$04.00/0

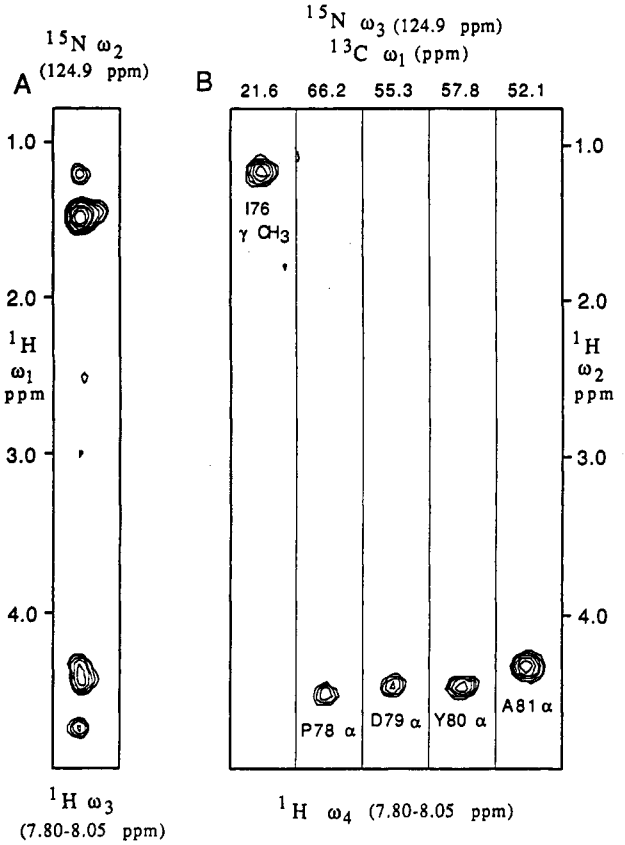

FIGURE 2: (A) ^{1}H(ω_1),^{1}H(ω_3) plane selected from a 3D [^{1}H,^{15}N,^{1}H] NOESY spectrum and (B) ^{1}H(ω_2),^{1}H(ω_4) planes from a 4D [^{13}C,^{1}H,^{15}N,^{1}H] NOESY spectrum of [U-^{15}N,^{13}C]FKBP/ascomycin in H_2O.

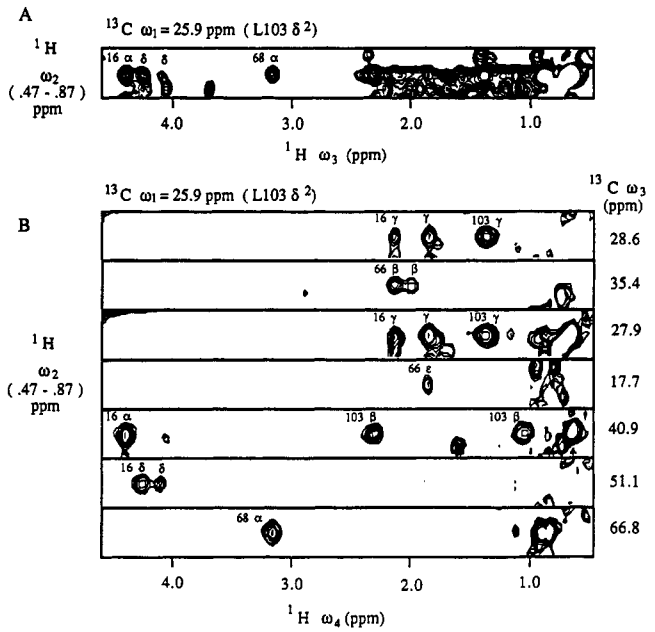

FIGURE 3: (A) ^{1}H(ω_2),^{1}H(ω_3) plane selected from a 3D HMQC-NOESY spectrum and (B) ^{1}H(ω_2),^{1}H(ω_4) planes from a 4D [^{13}C,^{1}H,^{13}C,^{1}H] NOESY spectrum of [U-^{15}N,^{13}C]FKBP/ascomycin in ^2H_2O.

two NMR structures of uncomplexed FKBP in solution (Michnick et al., 1991; Moore et al., 1991) except for residues 34–44 and 78–90. In contrast to the X-ray structures, these two regions were not well-defined by the NMR data and were thought to be flexible in solution. From a comparison of the ^{1}H and ^{15}N chemical shifts of uncomplexed FKBP and FKBP with bound FK506, it was postulated that significant changes in these loop regions occur upon drug binding and that the distinct inhibitory effects that result from FK506 and rapamycin binding may involve their influence on the geometry of these loops (Michnick et al., 1991).

Although three-dimensional structures of FKBP/immunosuppressant complexes have been determined by X-ray crystallography, no solution structure of such a complex has been reported. It is important to obtain solution structures of these complexes since conformational differences may exist in solution versus the crystalline state (Kline et al., 1988; Nettesheim et al., 1988; Clore & Gronenborn, 1991a), especially for regions that are involved in crystallographic contacts. Indeed, crystal contacts have been observed for several regions of an FKBP/FK506 complex (Van Duyne et al., 1993), and some of these portions of the complex may be important for binding to calcineurin.

From a computer-aided analysis of heteronuclear three-dimensional NMR spectra, we have recently reported (Xu et al., 1993) on the ^{1}H, ^{13}C, and ^{15}N assignments and secondary structure of FKBP when bound to the immunosuppressant ascomycin (Figure 1). Here, we present a high-resolution three-dimensional structure of the FKBP/ascomycin complex in solution that was generated from a total of 1958 experimental restraints derived from amide-exchange studies, heteronuclear 3D and 4D NOE data, and homo- and heteronuclear three-bond coupling constants obtained from multidimensional NMR spectra (Xu et al., 1992). Compared to other protein structures that have been obtained by NMR, only a few have been determined using such a large number of restraints (Kraulis et al., 1989; Qian et al., 1989; Omichinski et al., 1990; Clore et al., 1990a; Forman-Kay et al., 1991; Clore et al., 1991b) and only one using heteronuclear 3D and 4D NMR data (Clore et al., 1991b). The high-resolution structure of the FKBP/ascomycin complex in solution was compared to the NMR-derived structures of uncomplexed FKBP in solution and the X-ray structure of an FKBP/FK506 complex.

EXPERIMENTAL PROCEDURES

Sample Preparation. Recombinant human FKBP was cloned from a Jurkat T-cell cDNA library and expressed at high levels in *Escherichia coli* using translational coupling to the 5′ end of the *Escherichia coli kds*B gene (manuscript in preparation). [U-^{15}N]FKBP and [U-^{13}C,^{15}N]FKBP were purified from cells grown on a minimal medium containing [^{15}N]ammonium chloride alone or in combination with [U-^{13}C]-acetate (Venters et al., 1991), using ion-exchange and size exclusion chromatography (Edalji et al., 1992). The protein was concentrated to ~3 mM and exchanged into either a H_2O or ^2H_2O solution (pH = 6.5) containing potassium phosphate (50 mM), sodium chloride (100 mM), and dithiothreitol-d_{10} (5 mM). FKBP/ascomycin complexes (1/1) were prepared by incubating labeled FKBP with an excess amount of unlabeled ascomycin for 24–48 h at room temperature. The excess ascomycin was removed by centrifugation.

NMR. All NMR spectra were collected at 30 °C on Bruker AMX500 (500 MHz) and AMX600 (600 MHz) NMR spectrometers. NMR spectra were processed and analyzed using in-house written software on Silicon Graphics computers.

The ^{15}N-resolved 3D NOESY-HSQC experiment (Fesik & Zuiderweg, 1988; Marion et al., 1989) was acquired in eight scans per experiment with 160 (t_1) × 38 (t_2) × 1024 (t_3) complex points using spectral widths of 6173 Hz (ω_1, ^{1}H), 1773 Hz (ω_2, ^{15}N), and 8333 Hz (ω_3, ^{1}H). A NOESY mixing

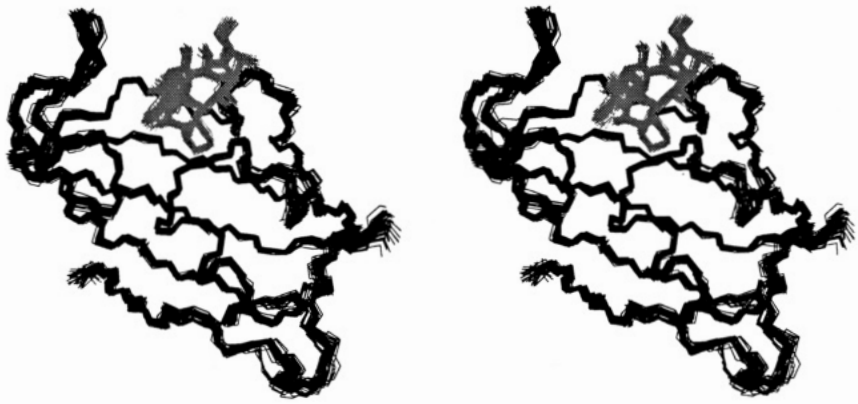

FIGURE 4: Stereoview showing the superposition of the C^{α}, C′, and N backbone atoms for the 43 solution structures of the FKBP/ascomycin complex. Ascomycin is shown in gray.

time of 50 ms was used, and water suppression was accomplished with a 2.5-ms spin-lock pulse using the method of Wüthrich and co-workers (Messerle et al., 1989).

The 4D [^{13}C, ^{1}H, ^{15}N, ^{1}H] NOESY spectrum (Kay et al., 1990) was acquired with eight scans per experiment with 12 × 80 × 10 × 512 complex points using sweep widths of 3289, 7463, 2128, and 10,000 Hz in ω_1 (^{13}C), ω_2 (^{1}H), ω_3 (^{15}N), and ω_4 (^{1}H), respectively. Water suppression was accomplished (Messerle et al., 1989) using two spin-lock pulses of 0.5- and 2.5-ms durations. The ^{13}C carrier frequency was set at 38 ppm. The regions from 70 to 49 ppm and from 27 to 5.5 ppm were folded once.

The 4D [^{13}C,^{1}H,^{13}C,^{1}H] NOESY spectrum (Zuiderweg et al., 1991; Clore et al., 1991b) was acquired with eight scans per experiment with 12 × 64 × 12 × 512 complex points using sweep widths of 3289, 5208, 3289, and 10 000 Hz in ω_1 (^{13}C), ω_2 (^{1}H), ω_3 (^{13}C), and ω_4 (^{1}H), respectively. The ^{13}C spectral widths were folded in the same manner as in the 4D [^{13}C,^{1}H,^{15}N,^{1}H] NOESY experiment. The ^{1}H carrier was centered at 3.7 ppm. For both 4D experiments a 10-ms homospoil was applied during the 50-ms NOESY mixing time to suppress unwanted magnetization, and a series of randomly spaced 90° pulses were used to saturate the ^{13}C spins at the very beginning of the pulse sequences (Clore et al., 1991b).

The 2D [^{1}H,^{13}C] HMQC spectrum (Müller, 1979) was acquired in $^{2}H_2O$ with 32 scans per experiment and 512 × 2048 complex points using sweep widths of 12 500 and 10 000 Hz in ω_1 (^{13}C) and ω_2 (^{1}H), respectively. The ^{13}C carrier frequency was set at 38 ppm. The 2D [^{1}H–^{15}N] HSQC (Bodenhausen & Ruben, 1980) spectrum was acquired in H_2O with 16 scans per experiment and 256 × 2048 complex points with sweep widths of 2128 Hz in ω_1 (^{15}N) and 2000 Hz and in ω_2 (^{1}H).

In order to determine the location of tightly bound water molecules, a ^{1}H–^{15}N ROESY-HMQC experiment (Clore et al., 1990b) was collected with eight scans per increment and a mixing time of 33 ms. The data set contained 96 (t_1) × 37 (t_2) × 1024 (t_3) complex points with spectral widths of 6024 Hz (ω_1, ^{1}H), 1773 Hz (ω_2, ^{15}N), and 8333 Hz (ω_3, ^{1}H). In addition, a ^{1}H–^{13}C NOESY-HMQC spectrum was collected with a mixing time of 50 ms on [U-^{13}C,^{15}N]FKBP dissolved in H_2O. The data set was collected with eight scans per experiment and consisted of 96 (t_1) × 48 (t_2) × 1024 (t_3) complex points, with spectral widths of 6024 Hz (ω_1, ^{1}H), 5747 Hz (ω_2, ^{13}C), and 8333 Hz (ω_3, ^{1}H).

NOE-Derived Distance Restraints. For FKBP, the proton–proton intramolecular distance restraints were derived from NOE data acquired from three different data sets. The NH/NH NOEs were obtained from a ^{15}N-resolved 3D NOESY-HSQC spectrum of [U-^{15}N]FKBP/ascomycin, the CH/NH NOEs were derived from a 4D [^{13}C,^{1}H,^{15}N,^{1}H] NOESY spectrum of [U-^{15}N,^{13}C]FKBP/ascomycin in H_2O, and the CH/CH NOEs were obtained from a 4D [^{13}C,^{1}H,^{13}C,^{1}H] NOESY spectrum of [U-^{15}N,^{13}C]FKBP/ascomycin in $^{2}H_2O$. From these three experiments, a total of 1575 distance restraints were obtained. Of these, 498 restraints (31.6%) were derived from intraresidue NOEs, 357 (22.7%) were from sequential NOEs, 177 (11.2%) were from short-range NOEs (between residues <5 amino acids apart in the sequence), and 543 (34.5%) were from long-range NOEs (≥5 residues apart). Distance restraints derived from NOEs for scalar-coupled protons were not included in the calculations if the restraint bounds were greater than the limits allowed by the covalent geometry. Standard pseudoatom distance corrections (Wüthrich et al., 1983) were added to account for center averaging, and NOE intensities for methyl groups were divided by 3 prior to the addition of a pseudoatom correction.

Distance restraints were obtained from NOE cross-peak volumes whose values were corrected to reduce the errors resulting from experimental artifacts. For protons attached to ^{15}N nuclei, such artifacts are primarily related to differences in amide relaxation rates which will affect the signal loss during the HSQC part of the 4D NOESY experiment. For protons attached to ^{13}C nuclei, anomalies in the observed NOE intensity may arise from differences in the transfer efficiency due to nonuniform scalar coupling, different transverse relaxation rates, and pulse rolloff errors. In order to correct for these errors, 2D HMQC (or HSQC) spectra were recorded under the same conditions as the HMQC or HSQC portion of the 4D NOESY experiment. Corrections were applied via the equation:

$$\mathrm{NOE}_{\mathrm{corrected}} = \mathrm{NOE}_{\mathrm{obs}}(I_{\mathrm{N}})^{-1}(I_{\mathrm{C}})^{-1} \qquad (1)$$

where $\mathrm{NOE}_{\mathrm{obs}}$ is the NOE intensity observed in the 4D NOE experiment, I_{N} is the integrated cross-peak volume from an ^{1}H–^{15}N HSQC spectra, and I_{C} is an averaged intensity correction applied to protons attached to ^{13}C nuclei (derived from integration of the ^{1}H–^{13}C HMQC spectrum). Volume integrals obtained from analysis of the ^{1}H–^{15}N HSQC spectrum were used directly in eq 1 as the I_{N} correction term. In cases of overlapping resonances in the ^{1}H–^{15}N HSQC spectra, an average of the values obtained for the well-resolved peaks was used. Unlike the well-resolved ^{1}H–^{15}N correlation spectra, the ^{1}H–^{13}C HMQC spectra contained significant overlap and thus precluded the use of explicit integrals for the I_{C} terms. Instead, an average intensity value for methine, methylene, and methyl protons was employed (1.0, 0.7, and

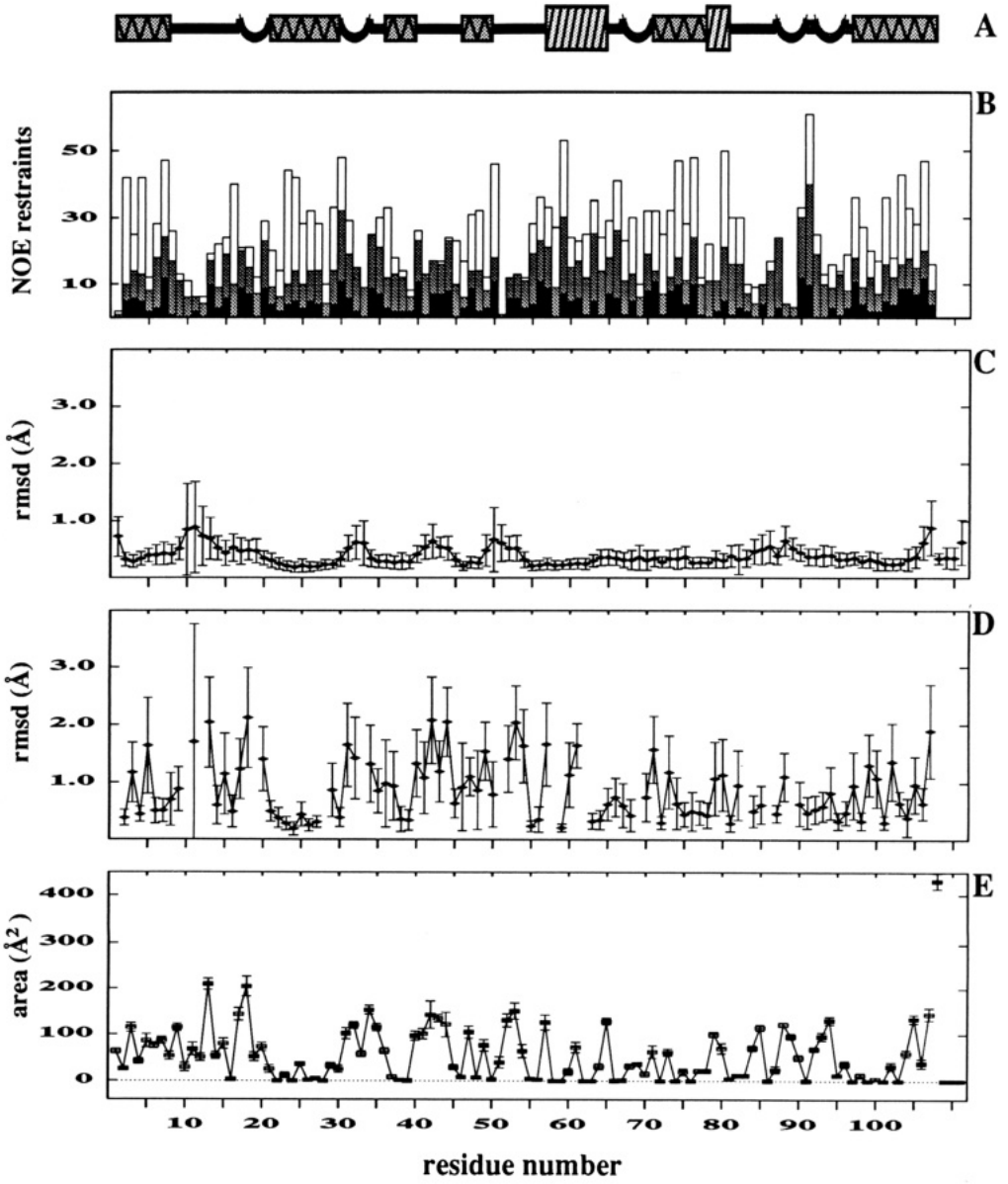

FIGURE 5: (A) Schematic representation of the secondary structure of FKBP in the FKBP/ascomycin complex in which lines denote loop regions, semicircles show either type I or type II β-turns, thin hatched boxes denote the positions of the β-strands, and the two large striped boxes depict the 3_{10} and α-helices. (B) Distribution of NOE restraints used in the structure calculations. The height reflects the total number of NOE-derived restraints for each residue while the black, gray, and white portions of the box correspond to the intraresidue restraints, the sum of sequential and short-range restraints, and the long-range restraints, respectively. The ligand had 50 intermolecular and 88 intraligand restraints and the 3 water molecules had 11 total NOE restraints. Residue-based root mean square deviations (Å) of the atomic coordinates from the mean atomic structure for (C) the backbone heavy atoms (C^{α}, C′, N, and O) and (D) all non-hydrogen atoms. (E) Residue-based solvent-accessible surface area (Å^2) calculated by using a 1.4-Å probe. In (C) and (E), ascomycin is depicted as residue 108, and the three water molecules are shown as residues 109, 110, and 111.

1.2, respectively). Classification of the corrected 4D NOE cross-peak volumes into distance ranges of 1.8–2.3, 1.8–2.7, 1.8–3.5, 2.2–4.2, and 2.4–5.0 Å produced the final set of FKBP intramolecular proton–proton distance restraints.

In addition to the intramolecular restraints for FKBP, 36 intermolecular and 88 intraligand distance restraints were obtained from a ^{13}C-resolved 3D HMQC-NOESY spectrum of [U-^{13}C]ascomycin bound to unlabeled FKBP acquired at 40 ms (Petros et al., 1991). An additional 14 intermolecular NOE-derived distance restraints were obtained from inspection of the 3D ^{1}H–^{13}C HSQC-NOESY spectrum. Intraligand and intermolecular NOEs were categorized into distance ranges of 1.8–2.7, 1.8–3.5, and 1.8–5.0 Å as indicated by a strong, medium, or weak NOESY cross-peak.

NOEs from the protein/ligand complex to water molecules were obtained from analysis of ^{1}H–^{13}C NOESY-HMQC and ^{1}H–^{15}N ROESY-HMQC spectra. A total of 11 distance restraints were obtained and given lower and upper bounds of 1.8 and 3.5 Å, respectively. A pseudoatom correction was added to the water molecules, resulting in a final upper bound of 4.5 Å.

Stereospecific Assignments and Torsional Angle Restraints. Stereospecific assignments of the Val γ-methyl and Leu δ-methyl groups of FKBP were obtained (Xu et al., 1993) using the method of Wüthrich and co-workers (Senn et al., 1989; Neri et al., 1989, 1990). The β-methylene protons for 45 residues were stereospecifically assigned from an analysis of the $^3J_{H^{\alpha},H^{\beta}}$ and $^3J_{N,H^{\beta}}$ coupling constants and relative NOE intensities as previously described (Xu et al., 1992).

Torsional angle restraints for 46 ϕ angles were obtained from coupling constants measured in a 2D HMQC–J spectrum (Kay & Bax, 1990) of [U-^{15}N]FKBP/ascomycin (Xu et al.,

Table I: Structural Statistics and rmsd for 43 FKBP/Ascomycin Structures[a]

structural statistics	⟨SA⟩	⟨$\overline{SA}$⟩r
rmsd (Å) from exptl distance restraints[b]		
all (1846)	0.015 ± 0.002	0.013
interresidue long (543)	0.009 ± 0.002	0.009
interresidue short (177)	0.016 ± 0.003	0.017
interresidue sequential (357)	0.013 ± 0.003	0.011
intraresidue (498)	0.019 ± 0.003	0.016
intraligand (88)	0.016 ± 0.001	0.018
intermolecular (50)	0.013 ± 0.002	0.010
hydrogen bonds (122)	0.014 ± 0.002	0.015
bound water (11)	0.001 ● 0.002	0.000
rmsd (deg) from exptl dihedral restraints (112)[c]	0.38 ± 0.05	0.29
selected XPLOR energies (kcal·mol^{-1})[d]		
E_{bond}	10.7 ± 0.7	9.4
E_{angle}	105.9 ± 4.7	100.7
$E_{improper}$	49.8 ± 1.5	47.8
E_{L-J}	−749.6 ± 10.9	−750.6
E_{cdih}	1.5 ± 0.4	0.9
E_{NOE}	20.6 ± 4.5	16.5
rmsd from idealized geometry used within XPLOR		
bonds (Å)	0.002 ± 0.00	0.002
angles (deg)	0.46 ± 0.01	0.47
impropers (deg)	0.62 ± 0.02	0.74

Cartesian coordinate rmsd (Å)	backbone	all non-H
⟨SA⟩ vs ⟨$\overline{SA}$⟩ all[e]	0.43 ± 0.08	0.80 ± 0.08
⟨SA⟩ vs ⟨$\overline{SA}$⟩ ascomycin[f]	na	0.32 ± 0.10
⟨$\overline{SA}$⟩ vs X-ray[g]	0.91 ± 0.09	1.44 ± 0.09
⟨$\overline{SA}$⟩r vs X-ray[g]	0.81	1.23

[a] ⟨SA⟩ is the ensemble of 43 final structures, ⟨$\overline{SA}$⟩ is the mean atomic structure obtained by averaging the superimposed coordinates for the 43 structures, and ⟨$\overline{SA}$⟩r is the energy-minimized mean atomic structure. [b] None of the structures had distance violations ≥0.3 Å. [c] None of the structures had angle violations ≥5.0°. [d] Energies were calculated by XPLOR using a square well potential for the NOE term (50 kcal·mol^{-1}·Å^{-2}) and a square well quadratic energy function for the torsional potential (200 kcal·mol^{-1}·rad^{-2}). E_{L-J} was calculated using the CHARMM (Brooks et al., 1983) empirical energy function and was included into the total empirical potential during the final 500 cycles of energy minimization. [e] Atomic rms deviation between the 43 NMR structures and the mean coordinates after superimposition of the backbone heavy atoms (includes the ligand ascomycin). [f] Atomic rms deviation of the ligand when only the protein atoms are least-squares fitted. The ligand maintains an intrinsic rmsd of 0.10 ± 0.06 Å. [g] Excludes the ligands.

1993). Experimental restraints were included for $^3J_{H^N,H^\alpha}$ coupling constants of less than 6.0 Hz as −50 ± 40° or greater than 9.0 Hz as −120 ± 40° (Pardi et al., 1984). Since $^3J_{H^N,H^\alpha}$ coupling constants of <6.0 Hz may reflect positive as well as negative ϕ angles (Pardi et al., 1984), restraints for these small values were included only if the residue was known to be in a helical region (Xu et al., 1993). Dihedral restraints for χ^1 angles were obtained from $^3J_{H^\alpha,H^\beta}$ and $^3J_{N,H^\beta}$ coupling constants measured from E.COSY-like spectra (Gemmecker & Fesik, 1991; Emerson & Montelione, 1992; Montelione et al., 1989) as previously described (Xu et al., 1992). A total of 66 χ^1 angle restraints were employed in the refinement, each with an allowed error of ±30°. Dihedral angle restraints for the heavy atoms of ascomycin were obtained directly from the energy-minimized averaged Cartesian coordinates for the reported structures of ascomycin when bound to FKBP (Petros et al., 1991). Error bars of ±30° were applied to the resulting dihedral angles. Since the intraligand dihedral angles were not strictly experimentally derived, they were not included in the total number of reported experimental restraints.

Hydrogen-Bonding Restraints. Slowly exchanging amide protons were identified from a series of HSQC spectra acquired over a period of several days (Xu et al., 1993). From these data and a visual inspection of the initial structures, 52 unambiguous hydrogen bond donor/acceptor pairs were identified and included as 104 HN → O (1.8–2.3 Å) and N → O (2.5–3.3 Å) restraints. Hydrogen bonds to the three tightly bound water molecules were identified from FKBP/water NOEs and from the locations of hydrogen bond donors and acceptors in the high-resolution NMR structures obtained without bound waters. The 18 hydrogen bonds thus identified were restrained to values of <2.5 Å (H → O) and 2.4–3.5 Å (N or O → O).

Strategy for Structure Refinement. In the first stage of structure refinement, the protein and ligand NOE restraints were given bounds of 1.8–5.0 Å, and a number of preliminary structures were calculated. The resulting coordinates were analyzed for unambiguous hydrogen bonds for the slowly exchanging amides and to correct the few inevitable assignment errors. The second stage of refinement then proceeded with the intraligand and intermolecular NOE-derived distance restraints, the corrected NOE-derived distances for the protein, the hydrogen bonds, and the dihedral angle restraints. The 50 structures produced from this round were of high quality and were used to position the water molecules for the final calculations which included all of the experimentally derived restraints and the three bound water molecules.

Structure calculations employed a distance geometry/dynamical simulated annealing (DG/SA) procedure (Nilges et al., 1988) and were carried out with the program XPLOR/DG (Brünger, 1988; Kuszewski et al., 1992) on a Silicon Graphics 4D-360 computer. In the first step of the refinement, the covalent geometry and experimental restraints were used in a distance geometry algorithm to generate a family of embedded substructures from a linear conformation of FKBP and a cyclic model for ascomycin. Embedded atoms included the backbone and β and γ heavy atoms of FKBP and all of the ligand heavy atoms. The remaining atoms were added by least-squares fitting to the embedded coordinates prior to the next step of the refinement procedure which consisted of high-temperature (2000 K) molecular dynamics followed by dynamical simulated annealing (Nilges et al., 1988). During this stage quadratic harmonic potentials were included for the covalent geometry, a square well quadratic term was used for the distance and dihedral restraints, and a simple quartic potential was employed from the van der Waals term (F_{repel}; Nilges et al., 1988). Force constants for the NOE-derived distance restraints were maintained at 50 kcal·mol^{-1}·Å^{-2} throughout the refinement process. Dihedral angle restraints were initialized to 5 kcal·mol^{-1}·rad^{-2} and increased to 200 kcal·mol^{-1}·rad^{-2} at the beginning of annealing. Annealing proceeded stepwise from 2000 to 100 K in 50 K decrements, with each step consisting of 0.25 ps of restrained molecular dynamics. The force constant on the repulsive term was increased stepwise during this phase to 4.0 kcal·mol^{-1}·Å^{-4} and was maintained at that value during the penultimate energy minimization which consisted of 1000 cycles of Powell minimization with the van der Waals hard-sphere radii set to 0.8 times the CHARMM values (Brooks et al., 1983). An additional 500 cycles of Powell energy minimization, which employed the full Lennard-Jones potential, produced the final structures.

RESULTS AND DISCUSSION

4D NOE Data. The excellent resolution afforded by the 4D NOE experiments allowed many NOEs to be unambiguously identified as illustrated in Figures 2 and 3. Figure 2A

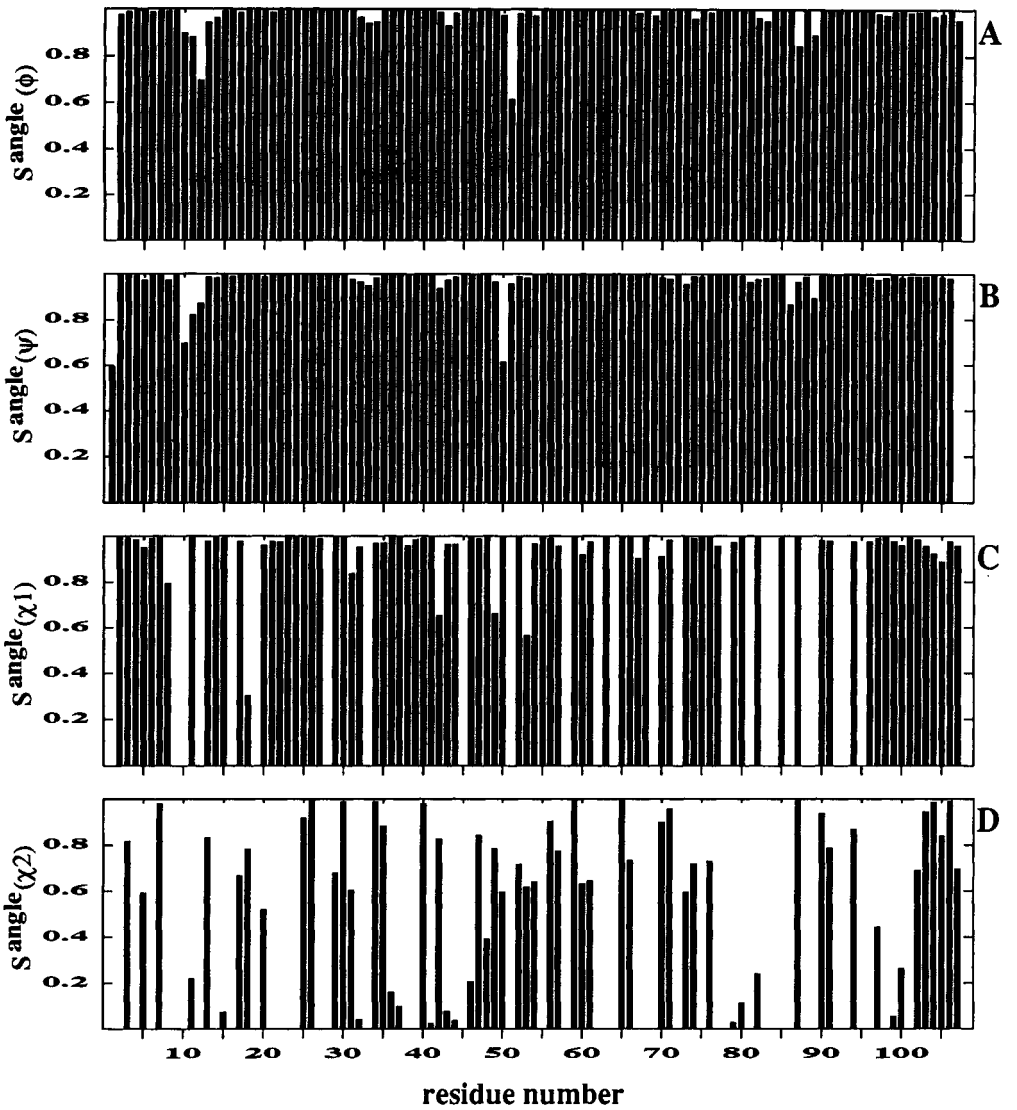

FIGURE 6: Angular order parameters, S^{angle}, for (A) ϕ, (B) ψ, (C) χ^1, and (D) χ^2 dihedral angles. Proline side-chain dihedral angles were not included in (C) and (D).

depicts a ^1H, ^1H plane extracted at the ^{15}N chemical shift of 124.9 ppm from a 3D ^{15}N-resolved NOESY-HSQC spectrum of the [U-^{15}N]FKBP/ascomycin complex. The NOE cross-peaks appear to be well resolved in the 3D data set. However, as shown in the ^1H,^1H planes extracted at the same ^{15}N frequency and different ^{13}C frequencies from the 4D-[^{13}C,^1H,^{15}N,^1H] NOE spectrum (Figure 2B), several H^N/H^α NOE cross-peaks that overlap in the 3D data are effectively resolved in the 4D NOESY spectrum. The spectral overlap problem is even more severe for NOEs between aliphatic protons. Although some NOEs can be resolved in ^{13}C-resolved 3D NOE spectra as illustrated in Figure 3A, many more NOEs are resolved and unambiguously identified in the 4D [^{13}C,^1H,^{13}C,^1H] data set (e.g., Figure 3B).

Quality of the FKBP/Ascomycin Structures. A superposition of the 43 NMR structures obtained from the DG/SA protocol is shown in Figure 4. Residue-based rms deviations for these structures are plotted in Figure 5, and the structural statistics are given in Table I. As shown in Table I, the NMR structures exhibit good covalent geometries and a large, negative VDW term, indicative of favorable nonbonded interactions. No structure showed NOE violations of >0.3 Å, and experimental torsion angles were all satisfied to within 5.0° of the applied bounds. The convergence of the FKBP/ascomycin structures was also analyzed using an elegant measure of torsion angle variability called the angular order parameter (S^{angle}) (Hyberts et al., 1992). In essence, S^{angle} reports on the deviation of a particular torsion angle between the limits of 0, corresponding to a random distribution of angles for that dihedral, and 1, in which all of the angles are identical. A plot of the calculated angular order parameters for the ϕ, ψ, χ^1, and χ^2 angles for FKBP in the FKBP/ascomycin complex in shown in Figure 6. It is important to note that, for residues that have symmetrically branched side chains such as Asp, Glu, Leu, Phe, Tyr, and Val, low values for S^{angle} may not always result from poor convergence. Instead, a 180° rotation of the side-chain atoms may produce two equally favorable yet out-of-phase populations with a near-zero S^{angle}. Analysis of the side-chain superpositions allows one to easily distinguish between random sampling of angle space and two equally populated 180° out-of-phase torsional angles.

As shown in Figures 4–6, the structures are well-defined by the NOE and dihedral angle restraints. Atomic rms deviations from the mean coordinates for the 43 structures were 0.43 ± 0.08 Å for the backbone heavy atoms (C^α, C′, N, O) and 0.80 ± 0.08 Å for all heavy atoms including the ligand and bound waters. Angular order parameters for ϕ and ψ backbone dihedrals had mean values of 0.98 and 0.97, respectively, indicating very good convergence for these

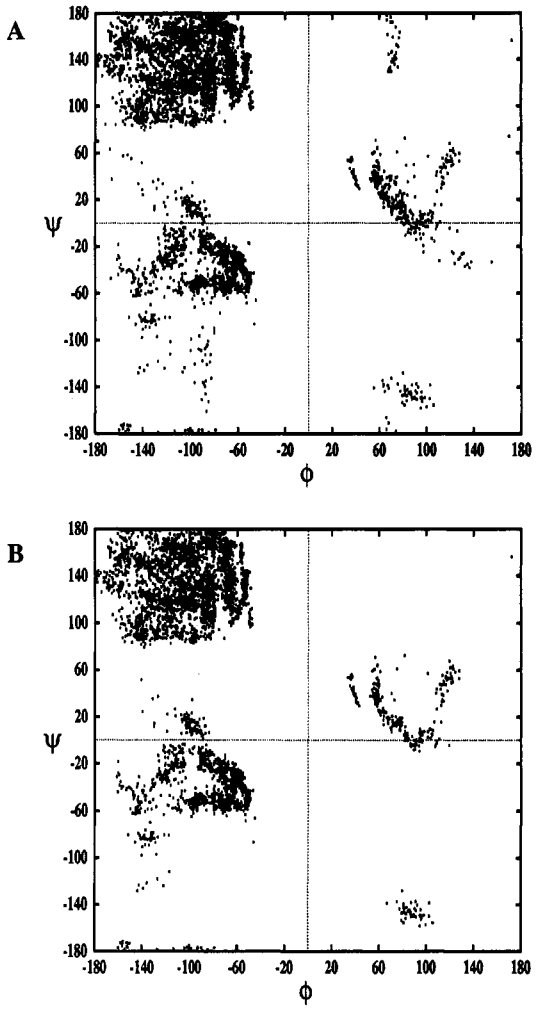

FIGURE 7: Ramachandran plots for the 43 NMR-derived solution structures of the FKBP/ascomycin complex (A) for all ϕ–ψ angles and (B) for those residues with ϕ and ψ S^{angle} >0.90 (97 residues).

torsional angles. A Ramachandran plot for the backbone angles for all 43 structures shows that most of the backbone geometries lie within energetically favorable regions of ϕ–ψ space (Figure 7A). Interestingly, three non-glycine residues, namely N43, Q53, and H94, exhibit positive ϕ angles in all of the 43 NMR structures. Although no dihedral restraint was applied to these angles, their observed $^3J_{H^N,H^\alpha}$ coupling constants of <6.5 Hz are fully consistent with positive ϕ angles (Pardi et al., 1984). Positive values for these three dihedrals were also observed in the X-ray structure of an FKBP/FK506 complex (Van Duyne et al., 1991a). Finally, the Ramachandran analysis is modestly improved (Figure 7B) if one includes only those angles that are well-defined by the NMR data, as judged by ϕ and ψ S^{angle} values >0.9. For FKBP, a total of 97 of the 105 ϕ–ψ pairs were above this cutoff.

Most of the β-strands in FKBP are amphipathic in nature [see also Rosen et al. (1991), Michnik et al. (1991), and Van Duyne et al. (1991a)], resulting in an interesting trend in the side-chain convergence. For example, as shown in Figure 8, well-defined side chains in β-strands I–V and the α-helix are observed for residues lining the hydrophobic core of the protein (side chains pointing toward the bottom of Figure 8), while less well defined side chains occur on the more solvent exposed face (side chains pointing toward the top of Figure 8). Heavy atom root mean square deviations for residues with internal side-chain atoms depicted in Figure 8 were 0.27 and 0.52 Å for the backbone and all heavy atoms, respectively. Such values indicate that these internal residues are very well-defined by the NMR data. For the residues with solvent-exposed side chains depicted in Figure 8, the heavy atom rms deviation was 0.86 Å, significantly higher than the internal side chains. Lysines and arginines were the least well defined of all FKBP residues, with atomic rms deviations for the backbone heavy atoms and all non-hydrogen atoms of 0.80 and 1.23 Å, respectively.

Finally, least-squares fitting of the ascomycin ligand, while ignoring the protein portion of the complex, resulted in a heavy atom rms deviation of 0.10 ± 0.02 Å, indicating that the ligand itself is well-defined. The orientation and position of the ligand within the binding pocket of FKBP are precisely defined by the intermolecular NOEs, as indicated by an rms deviation of 0.32 ± 0.10 Å for the ligand when only the backbone heavy atoms of the protein are superimposed.

Description of the Structure. As noted previously (Xu et al., 1993), the solution structure of FKBP in the FKBP/ascomycin complex consists primarily of five antiparallel β-strands and a single amphipathic α-helix. Inspection of the three-dimensional structure of the FKBP/ascomycin complex shows that the residues defining the β-strands are (I) 1–7, (II) 71–77, (III) 97–107, (IV) 21–29, (Va) 36–39, and (Vb) 46–49, while the amphipathic helix encompasses residues 57–64. A β-bulge is observed at residue 104, consistent with earlier studies of free FKBP in solution (Michnik et al., 1991; Rosen et al., 1991). Classical type I (residues 30–33), and type II (residues 17–20, 67–70, 87–90, 92–95) β-turns are also observed. A loop of well-defined, yet irregular structure is seen for residues 40–45 and serves to link β-strands Va and Vb. A single turn of a 3_{10} helix is observed for residues 78–80. The remainder of the protein consists primarily of loop regions.

Figure 9 depicts a ribbon diagram (Carson, 1987) of the solution structure of the FKBP/ascomycin complex. The folding topology for the right-handed twisting antiparallel β-strands is +3 + 1 −3 + 1 (Richardson, 1977), exactly as noted previously for uncomplexed FKBP (Rosen et al., 1991; Michnik et al., 1991) and the X-ray structure of the FKBP/FK506 complex (Van Duyne et al., 1991a; see this and the two preceding reference for a full discussion of FKBP's novel loop crossing topology). The resulting fold of the protein produces a hydrophobic binding pocket, lined with Tyr and Phe residues with a tryptophan (W59) positioned at the base.

The conformation of ascomycin is well-defined by the experimental data (see Table I) and, as expected, is essentially identical to the conformation as described in Petros et al. (1991). A total of 50 intermolecular NOEs between ascomycin and FKBP protein residues Y26, F36, F46, V55, I56, W59, Y82, H87, I90, I91, and F99 serve to position the ligand in the hydrophobic binding pocket (Figure 9). Calculations of the solvent-accessible area of ascomycin in the FKBP/ascomycin complex fully agree with our earlier experimental findings of solvent exposure determined from changes in proton relaxation rates of FKBP-bound ascomycin in the presence of a paramagnetic relaxation agent (Petros et al., 1992).

Intermolecular hydrogen bonds between ascomycin and FKBP serve to stabilize the position of the ligand. From exchange data and analysis of the structures derived without hydrogen bond restraints, we had determined that the amide of I56 participates in a hydrogen bond with the c1 lactone carbonyl of ascomycin (see Figures 1 and 9). On the basis of their close proximity in the NMR structures, additional hydrogen bonds were identified between the hydroxyl proton of Y82 and the c8 carbonyl oxygen of ascomycin and between the side-chain carboxyl of D37 and the c10 hydroxyl proton

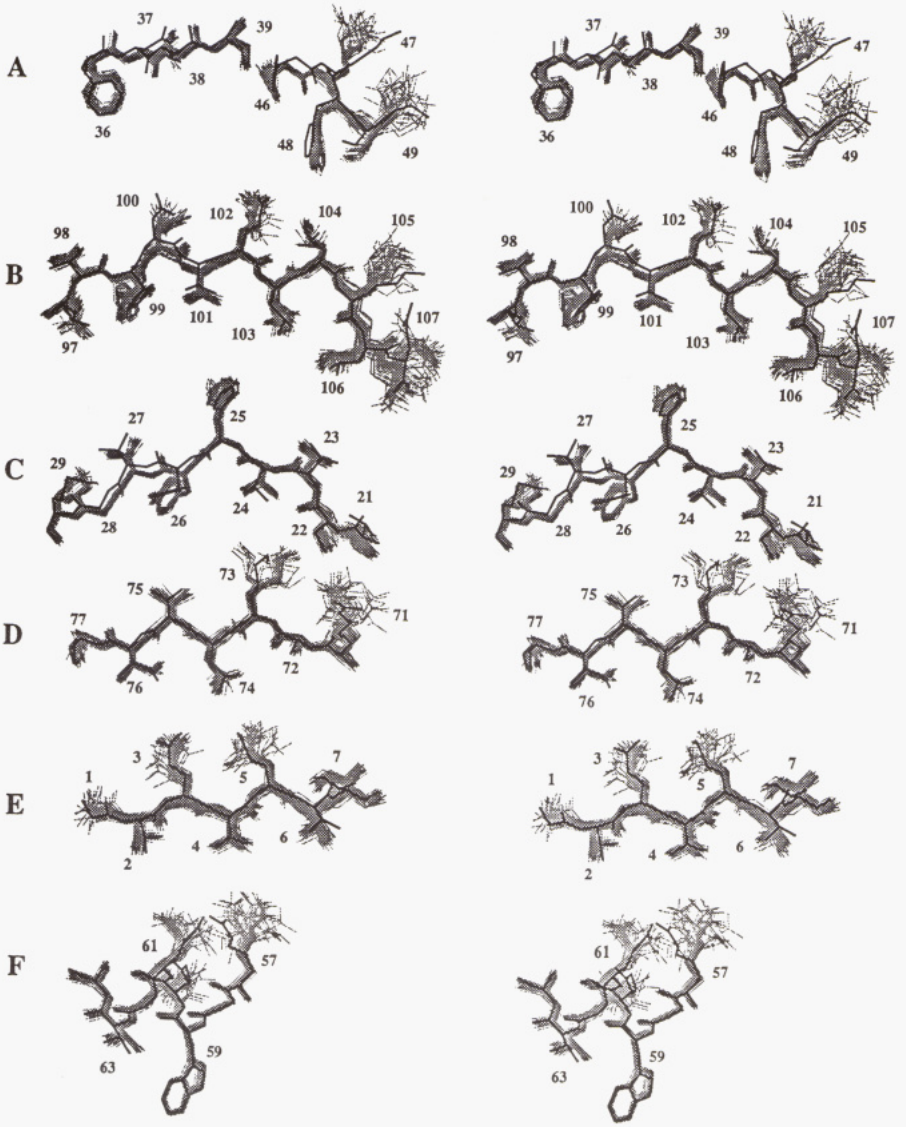

FIGURE 8: Stereoviews showing portions of the 43 FKBP/ascomycin structures (gray shaded) superimposed onto the mean atomic coordinates. Also shown is the local superposition of the X-ray structure (dark lines) of an FKBP/FK506 complex (Van Duyne et al., 1991a) onto the mean atomic coordinates. Highly solvent exposed residues are shown primarily on the upper face of each view, while residues with side chains projecting into the core of the protein/ligand complex are shown with side chains pointing toward the bottom of the figure for (A) β-strands Va and Vb, (B) β-strand IV, (C) β-strand III, (D) β-strand II, (E) β-strand I, and (F) the α-helix.

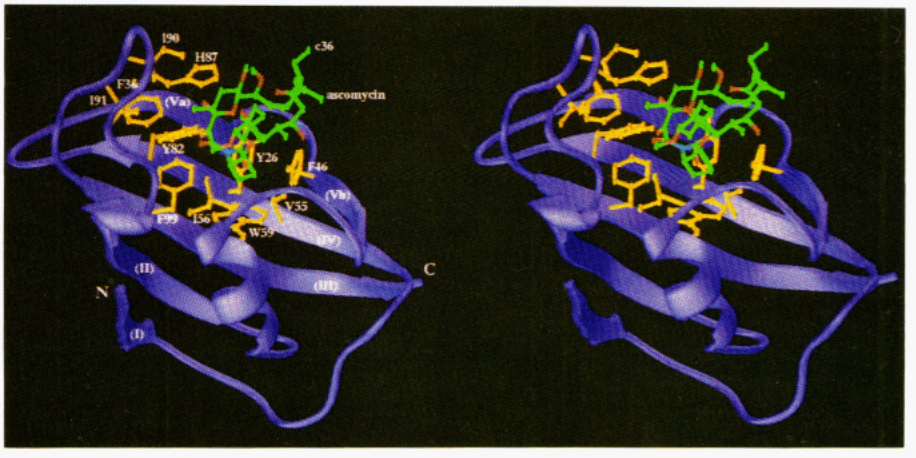

FIGURE 9: Stereoview ribbon diagram (Carson, 1987) of the FKBP/ascomycin complex. Side chains are shown in yellow and labeled for FKBP residues with NOEs to the ligand. Also labeled are ascomycin atom c36 and the five FKBP β-strands (I–V). Ascomycin is color coded by atom type with carbon atoms in green, oxygens in red, and the single nitrogen (N7) in blue.

of ascomycin. Also, as is noted in the crystallographic complex of FKBP/FK506, an interesting salt bridge triad (Van Duyne et al., 1993) which serves to stabilize two β-strands in the binding region (Va and Vb) is possible between Y26, D37, and R42. Although the mean distance to the guanidium group of R42 is quite long from both D37 and Y26, minimizations

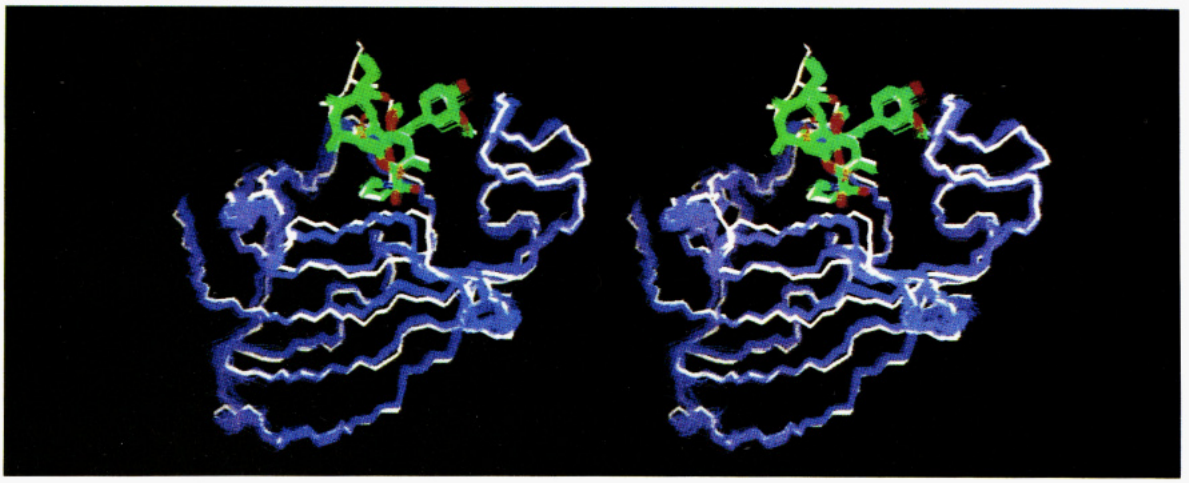

FIGURE 10: Stereoview of the 43 NMR-derived FKBP/ascomycin solution structures (blue) superimposed upon the X-ray structure of an FKBP/FK506 complex shown in white (Van Duyne et al., 1991a). Ascomycin is color coded by atom type with carbon atoms in green, oxygens in red, and the single nitrogen (N7) in blue. FK506 is shown in white.

with an R42 to D37 hydrogen bond restraint produce no additional NOE penalty, suggesting that such an interaction is consistent with our 1958 experimental restraints.

Comparison to NMR-Derived Structures of Uncomplexed FKBP. Two NMR-derived solution structures of uncomplexed FKBP have been reported (Moore et al., 1991; Michnik et al., 1991). Of these, one employed a total of 526 NOE-derived distance restraints and 64 hydrogen bonds to derive a low-resolution structure of bovine FKBP (Moore et al., 1991). Not surprisingly, from the paucity of distance restraints (less than 6 per residue), the rms deviations of the 20 reported structures were quite high: 3.1 Å for the backbone atoms and 3.7 Å for all non-hydrogen atoms. A second NMR solution structure of uncomplexed FKBP (Michnik et al., 1991; Rosen et al., 1991), based upon 910 NOE-derived distance restraints obtained from hetero- (^{15}N–^{1}H) and homonuclear 2D techniques, 50 hydrogen bond restraints, and 43 χ^1 and 44 ϕ angle restraints, resulted in rms deviations for 21 structures of 1.4 and 2.5 Å for backbone heavy atoms and all non-hydrogen atoms (excluding residues 83–90), respectively.

Although there is some slight disagreement in the exact placement and number of the elements, most of the secondary structures in the FKBP/ascomycin complex and uncomplexed FKBP are homologous to within ±1 residue. For example, the α-helix (residues 57–64) and β-strands I–IV were present in both the complexed and uncomplexed forms of FKBP. The β-bulge at L104 and the second part of strand III (residues 105–107), not reported by Moore et al. (1991), were identified in the reports of Michnik et al. (1991) and Rosen et al. (1991). The major differences in the free and bound forms of FKBP determined in solution were observed in residues 35–45 and 78–96. In neither structure of free FKBP was regular secondary structure observed for these regions of the molecule. Indeed, in both of the free structures, these regions were poorly defined and considered to be highly mobile (Michnik et al., 1991). In contrast, residues 36–39 are well-defined in the solution structure of the FKBP/ascomycin complex, adopting a β-strand conformation (Va) which is followed by a short section of well-defined (see Figure 5), yet irregular structure for residues 40–45. Additionally, although no ordered structure was observed for residues 78–92 in uncomplexed FKBP, in the FKBP/ascomycin complex, this section begins with a single turn of a 3_{10} helix (residues 78–80) and has two type II β-turns (residues 87–90 and 92–95).

It may be that some of the differences between the free and bound forms of FKBP are a result of differences in the

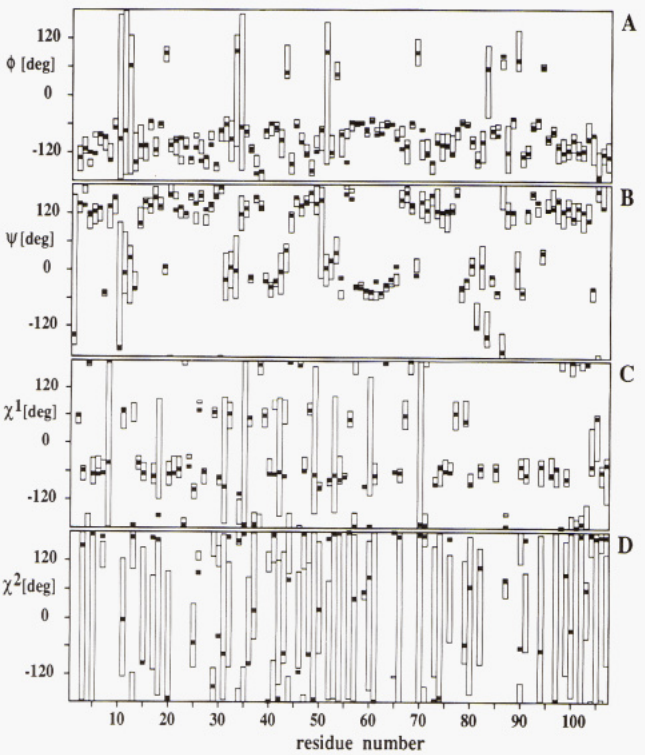

FIGURE 11: Plots of the (A) ϕ, (B) ψ, (C) χ^1, and (D) χ^2 dihedral angle ranges observed for the 43 FKBP/ascomycin structures (open boxes) against the values observed in the X-ray structure (dark boxes) of the FKBP/FK506 complex (Van Duyne et al., 1991a,b).

resolution of the structures. Earlier NMR-derived solution structures of uncomplexed FKBP were obtained from a smaller number of experimental restraints. With fewer restraints, the structures may simply have lacked the detail necessary for unambiguous analysis of the secondary structure. By using isotope labeling strategies and 3D and 4D NMR techniques, we were able to clearly assign and quantitate a much larger number of NOE restraints, resulting in highly refined structures. Alternatively, differences in the structures of the complexed and uncomplexed forms of FKBP may be due to stabilizing interactions between the ligand and the protein. As stated earlier, several intermolecular hydrogen bonds are observed in the FKBP/ascomycin complex, one of which involves the side-chain carboxyl of D-37 and the c10 hydroxyl of ascomycin (Figure 1). This hydrogen bond may be

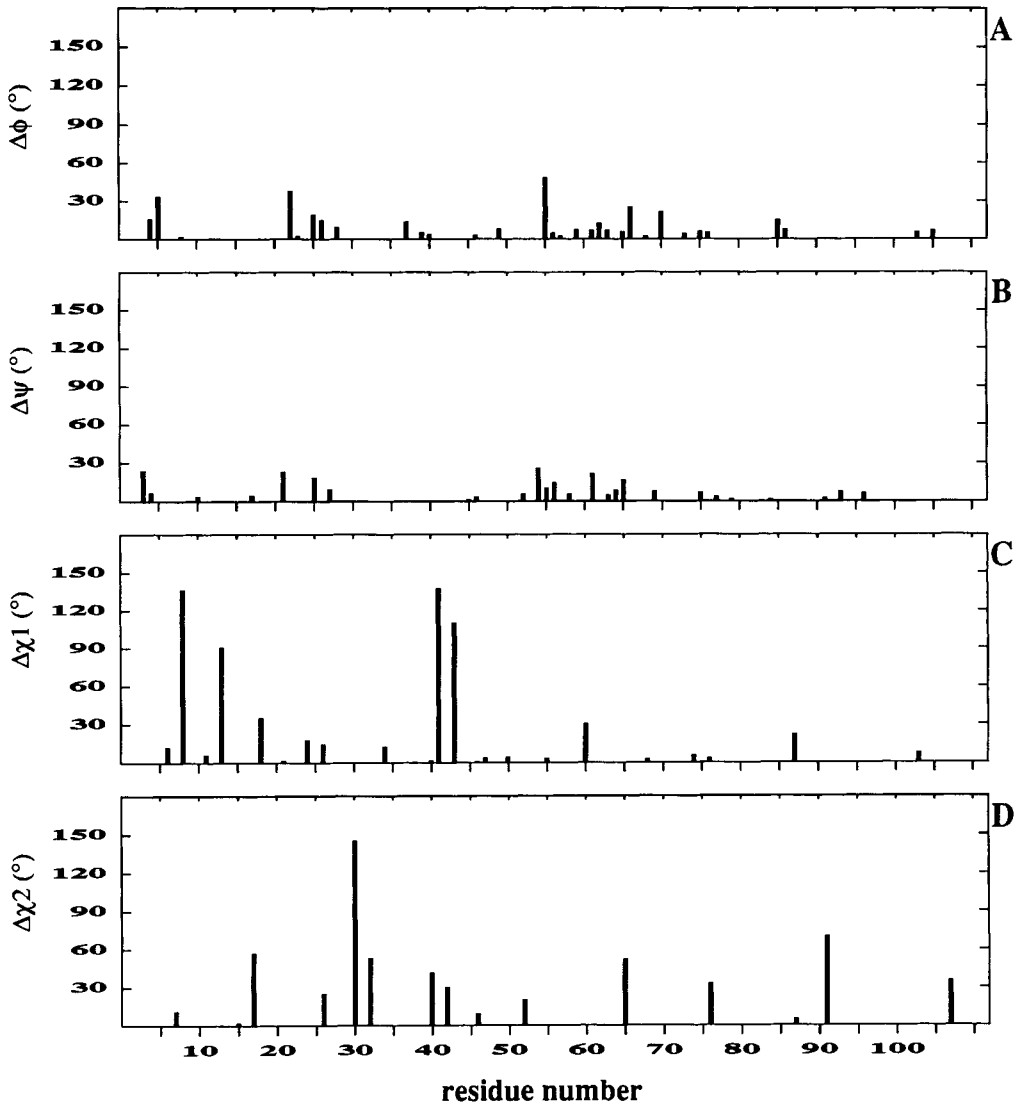

FIGURE 12: Deviations between the (A) ϕ, (B) ψ, (C) χ^1, and (D) χ^2 dihedral angles for FKBP in the FKBP/FK506 (X-ray) and FKBP/ascomycin (NMR) complexes. Deviations are calculated as the difference from the X-ray value to the nearest angular minimum or maximum observed for the NMR structures.

important in initiating the formation of, or stabilizing, the β-strand observed for residues 36–39, which was not observed in the NMR studies of uncomplexed FKBP. The loop region comprised of residues 78–95, which is ill-defined in the unbound form of FKBP, is stabilized by an intermolecular hydrogen bond involving the hydroxyl of Y82 and the c8 carbonyl of ascomycin and by a number of hydrophobic interactions (e.g., I90, I91, and F36; see Figure 9).

Comparison to the X-ray Structure of the FKBP/FK506 Complex. A plot of the ligand heavy atoms and FKBP C^{α}, C′, and N backbone atoms from the X-ray structure of FKBP/FK506 (Van Duyne et al., 1991a) is shown in Figure 10 (white) superimposed upon the NMR-derived solution structures of the FKBP/ascomycin complex (blue). As shown in the figure, most of the X-ray structure falls within the conformations sampled by the NMR data. Also, the two ligands appear to be well aligned, with modest differences observed for the most solvent exposed atoms of FK506 and ascomycin. Atomic rms deviations between the X-ray and the 43 NMR structures are 0.92 ± 0.09 Å for the backbone heavy atoms and 1.42 ± 0.09 Å for all non-hydrogen atoms (excluding the ligands). The deviation between the averaged, energy-minimized NMR and the X-ray structures is even smaller: 0.82 Å for the backbone heavy atoms and 1.30 Å for all FKBP heavy atoms.

Detailed evidence for the similarity in the backbone conformation of the solution and X-ray structures is obtained from comparisons of the backbone dihedral angles. In Figure 11, the ranges observed for the backbone and side-chain dihedral angles in the family of 43 NMR structures are shown along with the corresponding angles from the X-ray structure of the FKBP/FK506 complex. As shown in Figure 11, most of the ϕ and ψ angles are tightly clustered in the NMR conformations and have ranges that encompass the X-ray values. For those backbone angles that do not include the X-ray values, most deviate less than 20° from the X-ray structure (Figures 12A,B), and all of the ϕ and ψ angle ranges are within 50° of the X-ray values (although no ψ angles were included in the structure calculations). As noted earlier, positive ϕ angles are observed in both the X-ray and NMR structures for N43, Q53, and H94 (Figure 11).

Additional evidence for the similarity of the backbone conformation in the NMR and X-ray structures comes from comparing the distances of the NOE-derived restraints to the distances measured directly from the X-ray structure of the FKBP/FK506 complex (protons added by XPLOR). Of the 1575 NOE-derived distance restraints between FKBP protons, only 36 differed by more than 0.35 Å from the distances in the X-ray structure, and no difference was greater than 1.6

Å. Of the 36 distance violations, only 3 involved backbone–backbone interactions.

Similarity between the X-ray structure of FKBP/FK506 and solution structure of FKBP/ascomycin extends to many of the side chains, especially for side chains projecting into the core of the protein/ligand complex. Shown in Figure 8 are portions of the X-ray structure of FKBP/FK506 superimposed onto the 43 NMR solution structures of FKBP/ascomycin. As can be seen, nearly all of the internal side chains (shown pointing toward the bottom of the figure) have similar conformations in the two complexes. Examination of the side-chain dihedral angles (Figure 11) confirms that the χ^1 angles are tightly clustered and are often very similar in the NMR and X-ray structures (although the χ^2 angles were not nearly as converged as the other reported dihedral angles). As shown in Figures 11 and 12, only a very few χ^1 angles differ substantially between the structures of the complexes determined in solution or in the crystalline state.

Despite the striking similarities between the X-ray and NMR structures of these two complexes, differences between the X-ray structure of FKBP/FK506 and solution structure of FKBP/ascomycin are observed. Specifically, many of the highly solvent exposed side chains were unable to sample the conformation observed in the X-ray structure (Figure 8). Differences in the NOE-derived distance restraints show that, for the 36 distance violations described above, 17 were from lysine and arginine side chains and the remainder were primarily from other highly solvent exposed residues. As shown in Figure 12C, the χ^1 angles of S8, R13, D41, and R43 deviate substantially from the X-ray values. Likewise, D32, R42, and I91 have χ^2 angles that are dissimilar in the NMR and X-ray structures of FKBP/ascomyin and FKBP/FK506 (Figure 12D). Since many of these residues have fewer than the mean number of NOEs and also exhibit distortions in the X-ray conformation from numerous crystal contacts (Van Duyne et al., 1992), it is not unexpected to observe such differences. Additionally, some of the side chains observed in the X-ray structure to be involved in salt bridges (D41–K35, R40–D102, R42–D37, and E107–K47) are not well reproduced in the NMR solution structures.

Finally, L30, a nonsurface residue with no crystal contacts (Van Duyne et al., 1993), has the largest deviation in χ^2 between the NMR and X-ray structures. However, the conformation of L30 appears to be highly converged in the 43 NMR solution structures, with a χ^2 S^{angle} value of 0.98 and an atomic rms deviation of 0.40 Å for all heavy atoms. One explanation for the observed deviation in χ^2 angles is that there is an intrinsic difference between the X-ray and NMR conformations for L30. An alternative explanation is that Cδ1 and Cδ2 methyl groups of L30 are stereochemically incorrect in the X-ray structure. Interestingly, reversal of these methyls in the X-ray structure produces a side-chain conformation that is completely consistent with both our NMR and chemical data and reduces the angular deviations and NOE distance violations for L30 to zero.

CONCLUSIONS

We have reported on the 3D and 4D NMR-derived structure of the FKBP/ascomycin complex in solution. Root mean square deviations and angular order parameters show the 43 structures to be highly converged. The structure of the complex in solution differs from unbound FKBP for residues 35–45 and 78–92, yet is only modestly different from the crystallographic complex of FKBP/FK506, with differences mainly in highly solvent exposed side chains or residues involved in numerous crystal contacts.

ACKNOWLEDGMENT

We thank Tami Pilot-Matias and Steve Pratt for the cloning and expression of FKBP, as well as Tom Perun, George Carter, and Jay Luly for their support and encouragement. We also thank J. Clardy for providing a preprint of the manuscript describing the crystal contacts in the FKBP/FK506 complex.

REFERENCES

Bierer, B. E., Somers, P. K., Wandless, T. J., Burakoff, S. J., & Schreiber, S. L. (1990) *Science 250*, 556.
Bodenhausen, G., & Ruben, D. J. (1980) *Chem. Phys. Lett. 69*, 185.
Brooks, B. R., Bruccoleri, R. E., Olafson, B. D., States, D. J., Swaminathan, S., & Karplus, M. (1983) *J. Comput. Chem. 4*, 187.
Brünger, A. T. (1988) *XPLOR Manual*, Yale University, New Haven, CT.
Carson, M. (1987) *J. Mol. Graphics 5*, 103.
Clore, G. M., & Gronenborn, A. M. (1991a) *J. Mol. Biol. 217*, 611.
Clore, G. M., & Gronenborn, A. M. (1991b) *Science 252*, 1390.
Clore, G. M., Apella, E., Yamada, M., Matsushima, K., & Gronenborn, A. M. (1990a) *Biochemistry 29*, 1689.
Clore, G. M., Bax, A., Wingfield, P. T., & Gronenborn, A. M. (1990b) *Biochemistry 29*, 5671.
Edalji, R., Pilot-Matias, T. J., Pratt, S. D., Egan, D. A., Severin, J. M., Gubbins, E. G., Smith, H., Park, C. H., Petros, A. M., Fesik, S. W., Luly, J., Burres, N. S., & Holzman, T. F. (1992) *J. Protein Chem. 11*, 213.
Emerson, S. D., & Montelione, G. T. (1992) *J. Am. Chem. Soc. 114*, 354.
Fesik, S. W., & Zuiderweg, E. R. P. (1988) *J. Magn. Reson. 78*, 588.
Forman-Kay, J. D., Clore, G. M., Wingfield, P. T., & Gronenborn, A. M. (1991) *Biochemistry 30*, 2685.
Fung, J. J., Allesiani, M., Abu-Elmagd, K., Todo, S., Shapiro, R., Tzakis, A., Van Thiel, D., Armitage, J., Jain, A., McCauley, J., Selby, R., & Starzl, T. E. (1991) *Transplant. Proc. 23*, 3105.
Gemmecker, G., & Fesik, S. W. (1991) *J. Magn. Reson. 95*, 208.
Harding, M. W., Galat, A., Uehling, D. E., & Schreiber, S. L. (1989) *Nature 341*, 758.
Hyberts, S. G., Goldberg, M. S., Havel, T. F., & Wagner, G. (1992) *Protein Sci. 1*, 736.
Kay, L. E., & Bax, A. (1990) *J. Magn. Reson. 86*, 110.
Kay, L. E., Clore, G. M., Bax, A., & Gronenborn, A. M. (1990) *Science 249*, 411.
Kline, A. D., Braun, W., & Wüthrich, K. (1988) *J. Mol. Biol. 204*, 675.
Kraulis, P. J., Clore, G. M., Nilges, M., Jones, T. A., Petterson, G., Knowles, J., & Gronenborn, A. M. (1989) *Biochemistry 28*, 7241.
Kuszewski, J., Nilges, M., & Brünger, A. T. (1992) *J. Biomol. NMR 2*, 33.
Liu, J., Farmer, J. D., Jr., Lane, W. S., Friedman, J., Weissman, I., & Schreiber, S. L. (1991) *Cell 66*, 807.
Marion, D., Kay, L. E., Sparks, S. W., & Torchia, D. A. (1989) *J. Am. Chem. Soc. 111*, 1515.
Messerle, B. A., Wider, G., Otting, G., Weber, C., & Wüthrich, K. (1989) *J. Magn. Reson. 85*, 608.
Michnick, S. W., Rosen, M. K., Wandless, T. J., Karplus, M., & Schreiber, S. L. (1991) *Science 252*, 836.
Montelione, G. T., Winkler, M. E., Rauenbuehler, P., & Wagner, G. (1989) *J. Magn. Reson. 82*, 198.
Moore, J. M., Peattie, D. A., Fitzgibbon, M. J., & Thomson, J. A. (1991) *Nature 351*, 248.
Müller, L. (1979) *J. Am. Chem. Soc. 101*, 4481.

Neri, D., Szyperski, T., Otting, G., Senn, H., & Wüthrich, K. (1989) *Biochemistry 28*, 7510.
Neri, D., Otting, G., & Wüthrich, K. (1990) *Tetrahedron 46*, 3287.
Nettesheim, D. G., Edalji, R. P., Mollison, K. W., Greer, J., & Zuiderweg, E. R. P. (1988) *Proc. Natl. Acad. Sci. U.S.A. 85*, 5036.
Nilges, M., Clore, G. M., & Gronenborn, A. M. (1988) *FEBS Lett. 229*, 317.
Omichinski, J. G., Clore, G. M., Apella, E., Sakaguchi, K., & Gronenborn, A. M. (1990) *Biochemistry 29*, 9324.
Pardi, A., Billeter, M., & Wüthrich, K. (1984) *J. Mol. Biol. 180*, 741.
Petros, A. M., Gampe, R. T., Jr., Gemmecker, G., Neri, P., Holzman, T. F., Edalji, R., Hochlowski, J., Jackson, M., McAlpine, J., Luly, J. R., Pilot-Matias, T., Pratt, S., & Fesik, S. W. (1991) *J. Med. Chem. 34*, 2925.
Petros, A. M., Neri, P., & Fesik, S. W. (1992) *J. Biomol. NMR 2*, 11.
Qian, Y. Q., Billeter, M., Otting, G., Muller, M., Gehring, W. J., & Wüthrich, K. (1989) *Cell 59*, 573.
Richardson, J. S. (1977) *Nature 268*, 495.
Rosen, M. K., Michnick, S. W., Karplus, M., & Schreiber, S. L. (1991) *Biochemistry 30*, 4774.
Schreiber, S. L. (1991) *Science 251*, 283.
Senn, H., Werner, B., Messerle, B., Weber, C., Traber, R., & Wüthrich, K. (1989) *FEBS Lett. 249*, 113.
Siekierka, J. L., Hung, S. H. Y., Poe, M., Lin, C. S., & Sigal, N. H. (1989) *Nature 341*, 755.
Van Duyne, G. D., Standaert, R. F., Karplus, P. A., Schreiber, S. L., & Clardy, J. (1991a) *Science 252*, 839.
Van Duyne, G. D., Standaert, R. F., Schreiber, S. L., & Clardy, J. (1991b) *J. Am. Chem. Soc. 113*, 7433.
Van Duyne, G. D., Standaert, R. F., Karplus, P. A., Schreiber, S. L., & Clardy, J. (1993) *J. Mol. Biol.* (in press).
Venters, R. A., Calderone, T. L., Spicer, L. D., & Fierke, C. A. (1991) *Biochemistry 30*, 4491.
Wüthrich, K., Billeter, M., & Braun, W. (1983) *J. Mol. Biol. 169*, 949.
Xu, R. X., Olejniczak, E. T., & Fesik, S. W. (1992) *FEBS Lett. 305*, 137.
Xu, R. X., Nettesheim, D., Olejniczak, E. T., Meadows, R., Gemmecker, G., & Fesik, S. W. (1993) *Biopolymers* (in press).
Yoshimura, N., Matsui, S., Hamashima, T., & Oka, T. (1989) *Transplantation 47*, 351.
Zuiderweg, E. R. P., Petros, A. M., Fesik, S. W., & Olejniczak, E. T. (1991) *J. Am. Chem. Soc. 113*, 370.